eISSN 1981-1829

Ciência e Agrotecnologia
Science and Agrotechnology

Portable X-ray fluorescence sensor for ecofriendly, low-cost, and fast assessment of eucalypt charcoal attributes

Sensor portátil de fluorescência de raios-X utilizado em uma metodologia verde, barata e rápida para a análise de atributos de carvão vegetal de eucalipto

Renata Andrade[1], Lucas Benedet[1], Marcelo Mancini[1], Sérgio Henrique Godinho Silva[1], Camila da Silva Freitas[2], Marco Aurélio Carbone Carneiro[1], Nilton Curi[1*]

ABSTRACT

Brazilian steel industries require high-quality charcoal to produce pig iron. Desirable charcoal attributes include high elemental carbon content, large mean particle size (MPS), and high density, while producing low contents of ash and volatile matter, and presenting low contents of water and contaminants (e.g., phosphorous). These attributes are commonly determined by standardized laboratory analyses, which are time consuming and costly, besides generating chemical effluents. Portable X-ray fluorescence (pXRF) spectrometry can be used to avoid the downsides of laboratory analyses. The objective of this study was to evaluate the use of pXRF data in machine-learning models trained to predict attributes of eucalypt charcoal. pXRF data (elemental contents) from 276 charcoal samples were used to train predictive models using six machine-learning algorithms. Auxiliary explanatory variables (drying time, wood age, fine particle content, and friability) were included in the models. Models were trained to predict the following charcoal attributes: fixed C (%), ash content (%), volatile matter (%), MPS (mm), water content (%), density (kg/m^3), and P contents (%). Satisfactory predictions were obtained for volatile matter, MPS, moisture, and density ($R^2 > 0.6$), and very accurate predictions were obtained for ash and P contents ($R^2 > 0.75$). The inclusion of auxiliary explanatory variables increased the prediction accuracy of MPS (R2 increased from 0.61 to 0.82), bulk density (from 0.56 to 0.73), and P contents (from 0.86 to 0.94). These results indicate that pXRF can be used as an ecofriendly alternative to assess the quality of eucalypt charcoal utilized in metallurgy.

Index terms: Proximal sensors; pXRF; machine learning algorithms; metallurgy; waste minimization.

RESUMO

Indústrias metalúrgicas exigem carvão de alta qualidade para produzir ferro-liga. Os atributos desejáveis do carvão incluem alta porcentagem de carbono fixo, grande tamanho médio das partículas (MPS), alta densidade, baixa produção de cinzas e materiais voláteis, além de baixos teores de água e contaminantes. Esses atributos são determinados por análises laboratoriais padronizadas, que são demoradas e caras, além de gerarem efluentes químicos. A espectrometria de fluorescência de raios X portátil (pXRF) poderia ser usada para superar as desvantagens das análises laboratoriais. Este trabalho objetivou utilizar dados de pXRF em modelos de aprendizado de máquina treinados para predizer atributos de carvão de madeira de eucalipto. Os dados de pXRF de 276 amostras de carvão foram usados como variáveis explicativas para treinar os modelos preditivos usando seis algoritmos de aprendizado de máquina. Variáveis explicativas auxiliares também foram incluídas nos modelos. Os modelos foram treinados para predizer os atributos: C fixo, cinzas, matéria volátil, MPS, umidade, densidade e teor de P. Predições satisfatórias foram obtidas para matéria volátil, MPS, umidade e densidade ($R^2 > 0,6$), e predições muito exatas foram obtidas para os teores de cinzas e teores de P ($R^2 > 0,75$). A inclusão de variáveis explicativas auxiliares aumentou a acurácia da predição de MPS (R^2 aumentou de 0,61 para 0,82), densidade (de 0,56 para 0,73) e teores de P (de 0,86 para 0,94). Esses resultados indicam que o pXRF pode ser usado como uma alternativa ecologicamente amigável para avaliar a qualidade do carvão de eucalipto utilizado na indústria metalúrgica.

Termos para indexação: Sensores proximais; pXRF; aprendizado de máquina; metalurgia; minimização de resíduos.

Introduction

The steel industry is responsible for around 20% of the energy consumed by the industrial sector globally, and its main energy source is coal, which is used as a reducing agent (Mousa et al., 2016; Al Hosni et al., 2024). This concerns the environmental and energy sectors since coal is a non-renewable carbon source. Burning coal means releasing into the atmosphere high amounts of carbon formed during millions of years, which would otherwise remain stored underground. The steel industry is responsible for 7–9 % CO_2 emissions from fossil fuels, with an estimated total of 1.85 t CO_2/t steel (Holappa, 2020).

In Brazil, all coal consumed by the steel industry is imported (Sociedade de Investigações Florestais - SIF, 2020). In 2023, the country imported 18,104,029 t of coal, at a cost of 4,032.4 million dollars, of which 10,068,000 tons were bought by

Agricultural Sciences

Ciênc. Agrotec., 49:e026424, 2025
http://dx.doi.org/10.1590/1413-7054202549026424

Editor: Renato Paiva

[1]Universidade Federal de Lavras/UFLA, Departamento de Ciência do Solo/DCS, Lavras, MG, Brasil
[2]Pesquisadora Independente, Pojuca, BA, Brasil

*Corresponding author: ntcuri@gmail.com

Received in December 31, 2024 and approved in January 4, 2025

the steel industry (Empresa de Pesquisa Energética - EPE, 2023; Ministério da Indústria, Comércio Exterior e Serviços - MDIC, 2024). Given the high costs of coal importation and related environmental problems, Brazil began to invest in the production of iron alloy, steel, and pig iron using charcoal from Eucalyptus wood instead of non-renewable sources, contributing to the reduction of CO_2 net emissions (Instituto Brasileiro de Mineração - IBRAM, 2021; Protásio et al., 2021). Brazil is the world's largest producer of charcoal, reaching 7.0 million tons produced in 2021, almost all of it directed to the domestic market (Indústria Brasileira de Árvores - IBA, 2023). The amount of pig iron produced in Brazil using charcoal as a reducing agent in 2023 was 31.4 million tons, representing 24 % of the total production (Sindicato da Indústria do Ferro no Estado de Minas Gerais - SINDIFER, 2023). A total of 6.9 million tons of charcoal were obtained from planted forest wood, mainly from eucalypt (IBA, 2023; Oliveira et al., 2023). This shows importance of eucalypt to the industrial sector in Brazil and the development of research for improving the quality and homogeneity of the wood (Pereira et al., 2012). Therefore, to obtain high-quality charcoal, the chemical, physical, mechanical, and anatomical attributes of the wood must also be improved.

To produce high-quality metal alloys, the steel industry needs to use high-grade wood charcoal; that is, charcoal that has adequate physical and chemical attributes, to avoid compromising the integrity of the pig iron produced (Silva & Ataíde, 2019; Protásio et al., 2021). The desired attributes of high-grade wood charcoal include high contents of fixed carbon, large mean particle size (MPS), and high bulk density, while minimizing the production of ash and presenting low contents of water, volatile matter and phosphorus (P) (Pereira et al., 2012; Rodrigues et al., 2016; Santos et al., 2016; Carnaje et al., 2018; Dufourny et al., 2019; Protásio et al., 2019; Assis et al., 2020; Dias Júnior et al., 2021; Dong et al., 2022). To determine these attributes, charcoal samples must undergo laboratory analyses that require expensive equipment, chemical reagents, and trained professionals (American Society for Testing and Materials - ASTM, 2021). These analyses are time consuming and expensive, especially when applied to a large number of samples. Proximal sensors are an alternative which can facilitate these analyses (IBRAM, 2021; Protásio et al., 2021). Portable X-ray fluorescence (pXRF) spectrometry is an ecofriendly approach for providing clean, fast, and low-cost chemical characterization of different materials.

pXRF is a portable device capable of detecting and quantifying the total concentration in samples of multiple elements from Mg to U in the periodic table (Weindorf, Bakr & Zhu, 2014) and has the advantage of being easy and fast to use, requiring little (or no) sample preparation, in addition to being a non-destructive and clean analysis (Silva et al., 2021). The chemical characterization obtained with pXRF has been successfully used to train machine-learning models that can estimate chemical and physical attributes of a material of interest (Andrade et al., 2020; Benedet et al., 2020a; Rosin et al., 2022). Machine-learning models generated with pXRF data have been tested on different types of materials, such as soils, plant tissues, chemical and organic fertilizers, agricultural and non-agricultural lime, coal, biochar, among others, obtaining accurate estimations in many cases (Somprasong, Thiteja, & Jaroonpattanapong, 2018; Ward et al., 2018; Kagiliery et al., 2019; Faria et al., 2020; Zhou et al., 2020; Acquah et al., 2022; Dasgupta et al., 2022; Benedet et al., 2023; Andrade et al.; 2023a,b; Tomczyk & Larousse, 2024).

Given the scarcity of works evaluating charcoal attributes, this study proposes the use of pXRF with the aid of machine-leaning algorithms to predict chemical and physical attributes of charcoal used in metallurgy to enhance its quality control (fixed C, ash, volatile matter, MPS, moisture, density, and P contents). Additionally, the effect of auxiliary variables in the accuracy of prediction models was tested (drying time, wood age, fine particle content, and friability). We hypothesized that pXRF will be capable of providing accurate estimations of key charcoal attributes thus facilitating its quality control. We also expect that the inclusion of easily obtainable auxiliary data would improve the accuracy of predictive models.

Material and Methods

Sample collection

Samples of eucalypt charcoal (n = 276) were collected from the Brazilian Coastal Plains in the northern region of the Bahia State. These samples were obtained from the combustion of 19 different clones of *Eucalyptus spp*., grown in 49 different plots. An approximate volume of 200 L was collected in the pile formed after burning the wood in a rectangular furnace. The samples were divided into four containers of 50 L each (30x30x80 cm), arranged in a cross shape (one container at the center and the others spaced around it). From this arrangement, two diagonally opposite portions were removed, placed into a 100 L container, and sent to the laboratory for physical and chemical analyses. All subsequent analyses were conducted in samples from the 100 L container.

Laboratory Analyses

Particle size analysis was done by first passing the selected 100 L of charcoal through a series of sieves with different mesh sizes, separating it into different fractions (Table 1). Fine particle content was considered as the percentage of mass that passed through a 9.52 mm mesh. Friability was defined as the percentage of fine particles after compressing the samples. The fine particle mass used exclusively to calculate friability was obtained as follows: particles with diameter between 25.4 and 31 mm were compressed under a force of 1 ton for 1 minute; next, the compressed material was sieved with a 9.52 mm mesh and weighted. This procedure was repeated until approximately 60 g of the sample was retained

in the 80-mesh sieve. Bulk density was determined by measuring the mass and volume of sample containers.

Chemical analyses were done by proportionally sampling 1 kg from each fraction of the sieved charcoal, grounding it to powder, and passing the samples through 20- and 80-mesh sieves (0.841 and 0.117 mm, respectively). Samples were ground until 60 g remained in the sieve with 0.117 mm openings (80 mesh). Water content in the ground samples was measured by calculating the mass difference after heating 1 g of the sample at 105 °C and placing the sample in a desiccator until they reached room temperature. Next, samples were heated at 905 °C for 7 minutes and placed again in a desiccator until reaching room temperature. The mass difference was again calculated and used to estimate the content of volatile matter in samples. Lastly, samples were heated at 750ºC for six hours and dried. The residual mass was weighed and used to calculate the ash content. Fixed carbon content was calculated as the difference between volatile matter and ash content. P content was determined through inductively coupled plasma optical emission spectroscopy (ICP-OES) after digestion by nitric acid (HNO_3). The equations used to calculate physical and chemical attributes are shown in Table 1.

pXRF spectrometry analysis

Samples of eucalypt charcoal were ground and sieved (0.117 mm) and analyzed at the Environmental Geochemistry Laboratory of the Federal University of Lavras, in the State of Minas Gerais, Brazil. Analyses were performed using a Tracer 5g pXRF spectrometer (Analytical Instrumentation, Billerica, MA, USA), containing a Rh X-ray tube with 50 keV and 100 µA. Analyses were done via the inbuilt Geochem software in triplicate using the standard factory mode "*Plants*" for 30 s per beam, with a total scan time of 60 s for both beams for each sample (Weindorf & Chakraborty, 2018). Ground samples were added to a cylindrical cup covered with a Prolene film and mounted in the equipment. In total, the pXRF spectrometer detected the concentration of eleven elements in all samples: Si, P, Cl, K, Ca, Ti, Mn, Fe, Cu, Zn and Sr.

The accuracy of the equipment was assessed by calculating the recovery values using two reference samples: one certified by the pXRF manufacturer (CS-P), and the other certified by the National Institute of Standards and Technology (NIST) 1573a (tomato leaves). The recovery value (%) per element was calculated by: (content of the reference sample determined by pXRF/certified content) x 100 (Koch et al., 2017). The 11 elements used in this study presented the following recovery values (CS-P/1573a): Ca (89/75), Cl (–/71), Cu (–/125), Fe (–/131), K (85/73), Mn (102/119), P (80/57), Si (–/–), Sr (–/–), Ti (–/–), and Zn (102/184). Elements not detected by pXRF or not present in the reference materials are represented by dashes (–).

Statistical analyses and modeling

Boxplots and a Principal Component Analysis (PCA) (Jolliffe & Cadima, 2016) were used aiming to identify outliers and better characterize the dataset prior to the development of prediction models of eucalypt charcoal attributes (MPS, water content, volatile matter, ash content, fixed C, bulk density, and P content) based on pXRF data. The Spearman's correlation analysis was also conducted along with the PCA to investigate the pairwise relationship between variables. In addition to pXRF data, easily-obtained auxiliary data were used as explanatory

Table 1: Equations used to calculate physical and chemical attributes of eucalypt charcoal samples used as a reducing agent in metallurgy.

Attribute	Unit	Equation	Variables
Bulk Density	kg/m^3	$(M_1–M_2) / V$	M_1: mass of the full container (kg) M_2: mass of the empty container (kg) V: volume of the container (m^3)
Mean Particle Size	mm	[B(ac)+C(bd)+D(ce)+...+I(hj)+J(i-0)+100(j-0)]*0.005	a, b, c, d, ..., h, i, j: size of the mesh (mm)[1] A, B, C, D,..., H, I, J: accumulated percentages of particles
Friability	%	$(M_f/M_{charcoal}) * 100$	M_f: mass of compressed fine particles[2] $M_{charcoal}$: mass of the charcoal
Water Content	%	$[(M_w–M_d) / M_d] * 100$	M_w: wet sample mass M_d: dry sample mass
Volatile Matter	%	$[(M_i–M_f) / M_i] * 100$	M_i: initial dry sample mass M_f: final dry sample mass
Ash Content	%	$(M_r–M_s) * 100$	M_r: residual dry mass M_d: dry sample mass
Fixed C Content	%	100 – (VM+AC)	VM: volatile matter AC: ash content

[1]Mesh sizes in mm, from a to j: 100, 76.2, 64, 50, 38.1, 32, 19.1, 12.7, 9.52, 6.32. [2]particles that passed through the 9.52 mm mesh.

variables to train prediction models, including: drying time of the wood, wood age, fine particle content, and friability. Drying time is the number of days the wood was left drying in the field before being collected and turned into charcoal. Wood age is the age of the carbonized tree in years. Fine particle content was defined as particles that passed through the 9.52 mm sieve, and friability is the resistance of charcoal samples to compression, as described in the physical analyses (section 2.2).

Afterwards, the dataset was randomly separated into training and validation sub-datasets, consisting of 70% (n = 193) and 30% (n = 83) of the total samples, respectively. For each attribute, Recursive Feature Elimination (RFE) was used to select the optimal pXRF explanatory variables using the "Boruta" package (Kursa & Rudnicki, 2010). This method performs a top-down search for relevant features and ranks their importance. Based on results from RFE, the pXRF variables were classified as Confirmed (important feature), Tentative (feature that does not impact the model's accuracy) or Rejected (not important feature).

The prediction models (with or without auxiliary variables) were created using six different machine learning algorithms: Projection Pursuit Regression (PPR) (Friedman & Stuetzle, 1981), Partial Least Squares (PLS) (Frank & Friedman, 1993), Random Forest (RF) (Breiman, 2001), Support Vector Machine (SVM) (Cortes & Vapnik, 1995), Extreme Gradient Boosting (XGB) (Chen & Guestrin, 2016), and Cubist Regression (CR) (Kuhn et al., 2012). All the models were built in the R software, version 4.1.0 (R Development Core Team, 2021), using the "caret" package (Kuhn, 2008). The importance of variables (IncNodePurity) was determined by the mean reduction of accuracy when removing each variable from the model. The greater the increased error, the more important this variable is for the model (Breiman, 2001; Liaw &Wiener, 2002).

Evaluation of model performance

The accuracy of predicted charcoal attributes by the tested machine learning algorithms was performed by comparing predicted versus observed values through the coefficient of determination (R^2), root mean square error (RMSE) (Equation 1), and residual prediction deviation (RPD) (Equation 2). The equations are given below:

$$RMSE = \sqrt{\frac{1}{n}\sum_{i=1}^{n}\left(y_i - m_i\right)^2} \quad (1)$$

$$RPD = SD / RMSE \quad (2)$$

where, n is number of observations, y_i is the value estimated by the model, m_i is the value determined by chemical and physical analyses; and SD is the standard deviation of the observed values. RPD has been framed into three classes: RPD > 2, prediction models delivering accurate results, 1.4 ≤ RPD ≤ 2, prediction models providing moderately accurate results, and RPD < 1.4, prediction models being non-reliable (Chang et al., 2001). The models with greater R^2 and smaller RMSE are considered optimal for predicting laboratory analyses.

Relative error increase

The percentage of RMSE increase (RI) was calculated to compare the performance of the tested machine learning algorithms (Andrade et al., 2022; 2023a). RI was calculated by using the lowest RMSE value achieved by the most accurate model as a reference to assess the Relative Increase (RI) of RMSE (Equation 3). That is, the RMSE of the most accurate model was compared to the RMSE values from the other models to evaluate differences in prediction accuracy among models. The calculations were made by separating the models trained with or without the auxiliary variables and were also carried out by grouping all the models, allowing to evaluate whether the addition of the auxiliary variables contributed to the accuracy of the models. The RI Equation 3 follows below:

$$RI = \frac{RMSE_{compared} - RMSE_{mostaccurate}}{RMSE_{mostaccurate}} \times 100 \quad (3)$$

where, $RMSE_{most\ accurate}$ is the lowest RMSE value achieved by the model used as reference, and $RMSE_{compared}$ is the RMSE value achieved by the other models.

Results and Discussion

Descriptive statistics

The attributes of charcoal samples presented coefficient of variation (CV) > 50% for water, ash, and P contents (Table 2). The distribution of water content data presented many points above the third quartile (i.e., indicating a right-tailed distribution), with most values found close to zero percent (Figure 1). Fixed C showed a low CV (7.32 %), with values ranging from 59.08 to 91.13% (Table 2). The CV of MPS, volatile matter and bulk density showed intermediate values. The auxiliary variables drying time, wood age and friability also presented intermediate CV values, between 20 and 40% (Table 2). Conversely, water content presented the highest CV (121.18%).

Among the elements quantified by pXRF analysis, Ca and Cu data presented the lowest CV, below 30% (Table 3). Cu presented a small amplitude, ranging from 3 to 11 mg kg^{-1}. Conversely, Ti, Mn, Fe, and Zn presented CV values above 80 %, indicating high heterogeneity. The PCA analysis showed a strong relationship between water content and Fe contents determined by pXRF (Figure 2), which was corroborated by the correlations analysis (r=0.71, Figure 3), but the reasons behind this relationship are unknown. Ti,

Zn, and Si revealed shorter vectors in the direction of water content in the PCA (Figure 2) and were shown to be mildly correlated, with coefficients varying from 0.34 to 0.53. Friability and MPS were positively correlated (r=0.35), while fine particle content presented negative correlation with MPS (r=-0.73) (Figures 2 and 3). Ash content, Sr, and Ca vectors were very close in the PCA, indicating a strong relationship between these variables, which was supported by the correlation analysis (r=0.76). The same was observed between fixed C and P content, and among the variables P, K, and Cu. Drying time, wood age, and volatile matter were positively correlated with each other, but negatively correlated with fixed C and P content. The highest correlation was observed between volatile matter and fixed C, which presented almost a 1 to 1 negative relationship (r=-0.99) (Figure 3).

Table 2: Descriptive statistics of conventional chemical and physical laboratory analyses of eucalypt charcoal samples from wood collected at the Brazilian Coastal Plains, in the state of Bahia, Brazil.

Auxiliary variables					Eucalypt charcoal attributes						
Statistics	Drying time	Wood age	Fine particle content	Friability	MPS[1]	Water content	Volatile matter	Ash content	Fixed C	Bulk density	P content
				%	mm	%	%	%	%	kg/m³	%
Min	2.40	5.90	0.58	9.60	29.64	0.36	7.26	0.26	59.08	148.13	0.005
Max	16.50	17.40	16.67	31.68	77.48	65.19	39.78	3.97	91.13	393.08	0.030
Mean	5.62	8.44	4.39	18.83	57.34	7.89	21.10	1.30	77.58	229.13	0.013
Median	5.3	7.5	3.56	18.2	61.8	3.87	20.5	1.2	77.9	221	0.01
STD[2]	2.13	2.56	3.01	4.19	11.93	9.56	5.80	0.65	5.68	40.66	0.007
CV (%)[3]	37.82	30.31	68.56	22.27	20.80	121.18	27.50	50.03	7.32	17.74	51.188

[1]Average particle size; [2]Standard deviation; [3]Coefficient of variation.

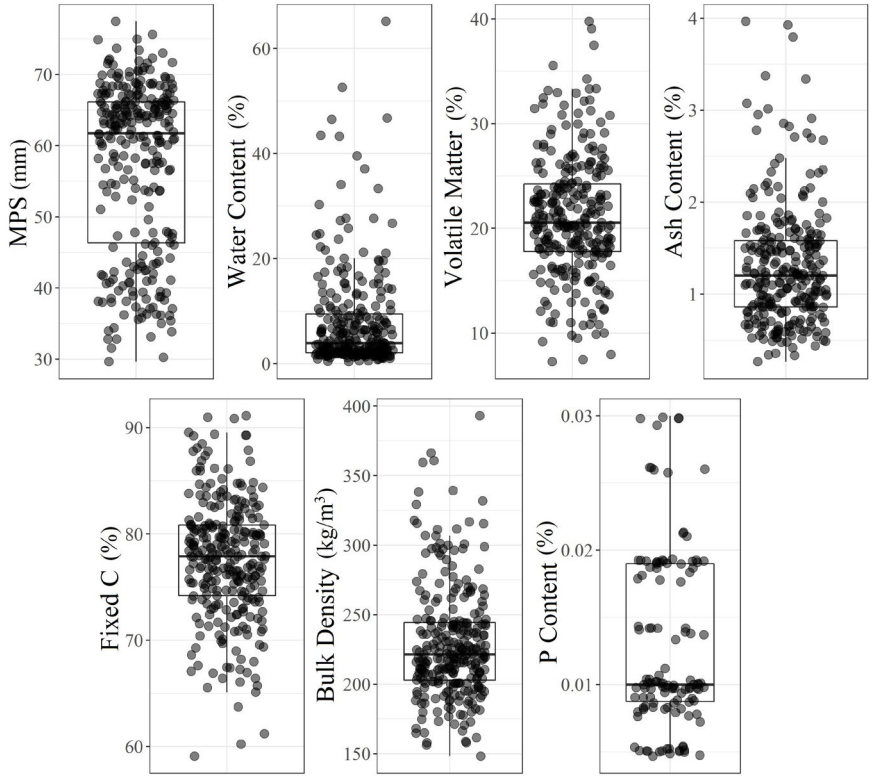

Figure 1: Boxplots of eucalypt charcoal attributes obtained by conventional laboratory analyses from samples collected at the Brazilian Coastal Plains, in the state of Bahia, Brazil. MPS – mean particle size.

Table 3: Descriptive statistics of portable X-ray fluorescence (pXRF) elemental data of eucalypt charcoal samples collected at the Brazilian Coastal Plains, in the state of Bahia, Brazil.

Statistic	Si	P	Cl	K	Ca	Ti	Mn	Fe	Cu	Zn	Sr
				mg/kg							
Min	270	0	0	0	2797	0	4	15	3	5	10
Max	5001	481	2059	4893	12541	43	192	1497	11	116	56
Mean	1476.8	200.7	575.2	1589.5	6859.4	6.3	35.1	192.3	5.7	15.7	25.5
Median	1366	194	458	1305	6606	5	26	106	6	11.5	24
STD[1]	751.9	76.0	402.3	1111.9	1829.6	6.8	29.9	222.3	1.2	13.0	9.5
CV (%)[2]	50.9	37.9	69.9	70.0	26.7	108.1	85.3	115.6	21.4	83.3	37.4

[1]Standard deviation;[2]Coefficient of variation.

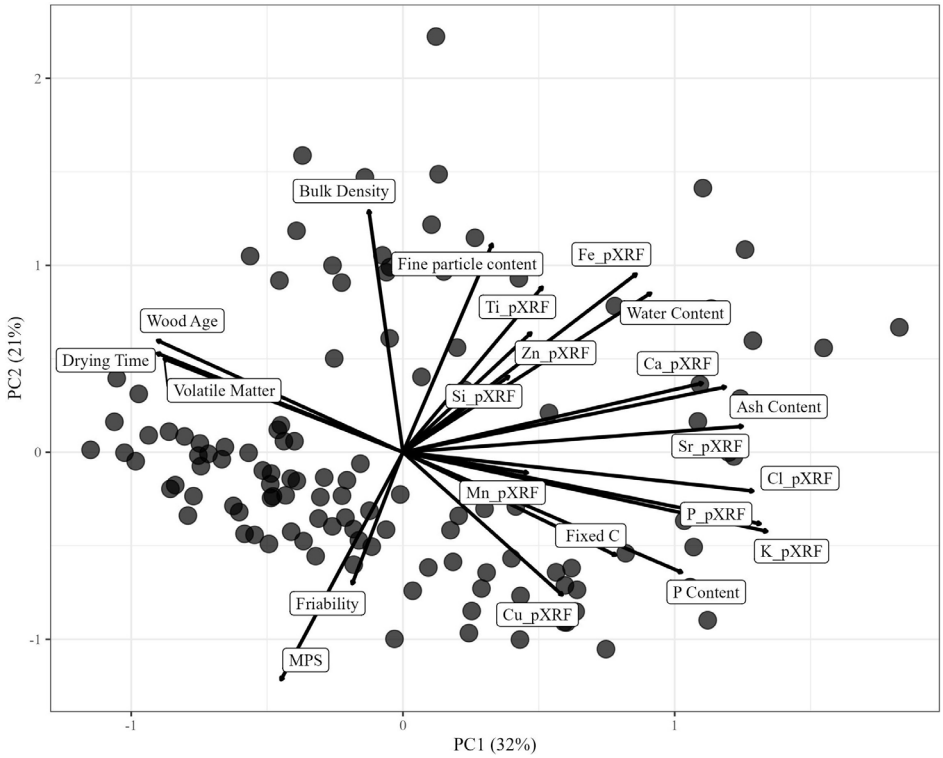

Figure 2: Principal Component Analysis (PCA) of eucalypt charcoal attributes and elemental contents obtained by portable X-ray fluorescence (pXRF) analysis from samples collected at the Brazilian Coastal Plains, in the state of Bahia, Brazil.

Prediction models

Using only pXRF data

The prediction performance of models is shown in Table 4. Predictions of fixed C showed low accuracy regardless of the machine-learning algorithm used. The highest R^2 value in these models was 0.42, achieved by the Cubist algorithm, and the lowest RMSE value was 4.22%, achieved by the XGB algorithm (Figure 4). Prediction models for volatile matter, MPS, moisture, and bulk density presented intermediate performance, whereby the best models for each attribute achieved R^2 values between 0.56 and 0.64 (Figure 4). RF was the best algorithm for predicting volatile matter and MPS, while Cubist was the best one for water content and bulk density. Ash and P contents presented the models with the best performances. The best algorithm to predict ash content was PPR, with an R^2 value of 0.75 (Figure 4). Prediction of P content achieved the best results, except for XGB and Cubist. The best model was built with the SVM algorithm, presenting the highest R^2 (0.86) and the lowest RMSE (0.0025%) (Figure 4). The performance of the PLS algorithm was also satisfactory, achieving R^2 of 0.82 and RMSE of 0.0031%.

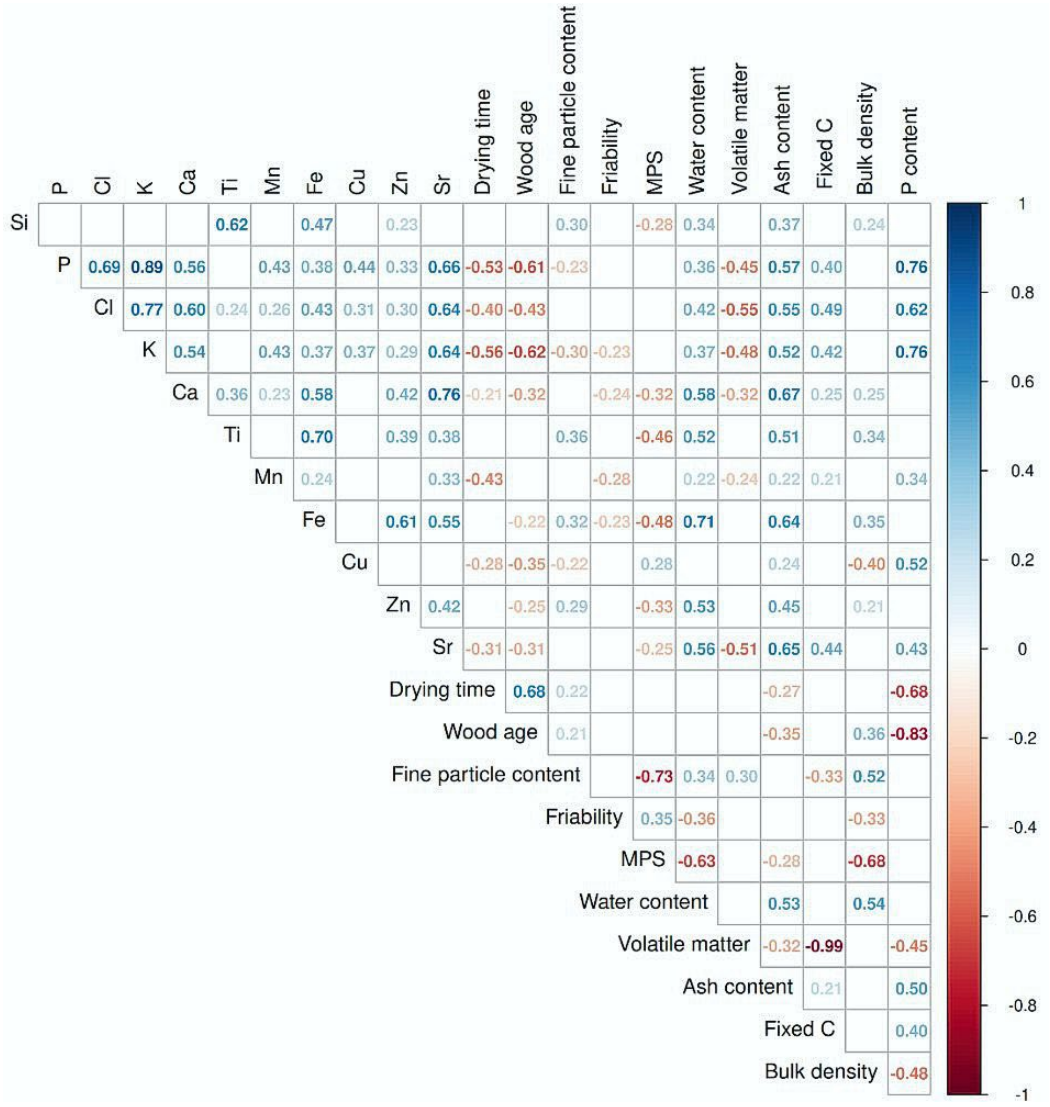

Figure 3: Spearman's correlation coefficients (r) of eucalypt charcoal attributes and elemental contents obtained by portable X-ray fluorescence (pXRF) analysis from samples collected at the Brazilian Coastal Plains, in the state of Bahia, Brazil. Blank squares indicate that coefficients were not statistically significant (p>0.05).

Fe content appeared five times in the selected group of important variables and was considered the most important for ash content, water content, and bulk density. Fe also was also ranked as the second most important variable for MPS. Ti appeared four times, being the most important variable for MPS and the second most important variable for ash content, water content, and bulk density. Cl was the most important variable for fixed C and volatile matter predictions, and K for P content predictions. Sr and P were also considered important by models, appearing four times among the most important variables.

Models trained with only pXRF data achieved high prediction accuracy for ash (PPR, R^2 = 0.75) and P content (SVM, R^2 = 0.86), reasonable accuracy for volatile matter, MPS, water content, and bulk density (R^2 = 0.56 to 0.64), but they could not provide accurate predictions for fixed C ($R^2 \leq 0.40$). Studies using pXRF to assess eucalypt charcoal are still incipient. Promising results were observed by Ward et al. (2018) in coal samples (coal cores and blocks), who found a good relationship ($R^2 \approx 0.90$) between total oxide contents and ash yield. In a related context, XRF data were able to distinguish charcoal from native species from that created from eucalyptus (Ramalho et al., 2020). Kagiliery et al. (2019) used a similar method to predict total S content in coal samples from four mines in North Dakota, USA, and likewise found that complementing pXRF data with other auxiliary variables such as color can improve predictions and facilitate the discrimination of the origin of coal samples.

Table 4: Root mean square error (RMSE), coefficient of determination (R^2), residual prediction deviation (RPD), and relative error increase (RI) for predictions of eucalypt charcoal attributes using portable X-ray fluorescence (pXRF) elemental data and auxiliary explanatory variables from samples collected at the Brazilian Coastal Plains, in the State of Bahia, Brazil. All metrics were calculated from validation data, unseen by models in the training phase.

		pXRF				pXRF + Auxiliary variables			
Variable	Model	RMSE	R^2	RPD	RI	RMSE	R^2	RPD	RI
Fixed C	PPR	4.26%	0.36	1.24	0.99	4.85%	0.34	1.22	12.55
	PLS	4.54%	0.27	1.17	7.59	4.74%	0.35	1.24	9.85
	RF	4.24%	0.35	1.25	0.59	4.38%	0.45	1.35	1.66
	SVM	4.71%	0.24	1.13	11.59	4.81%	0.34	1.22	11.65
	XGB	4.22%	0.4	1.26	0	4.31%	0.46	1.37	0
	CR	4.3%	0.42	1.23	2.1	4.63%	0.39	1.27	7.27
Ash Content	PPR	0.35%	0.75	1.99	0	0.41%	0.67	1.74	9.4
	PLS	0.46%	0.58	1.54	28.82	0.43%	0.66	1.69	12.29
	RF	0.41%	0.7	1.72	15.44	0.38%	0.74	1.9	0
	SVM	0.41%	0.67	1.74	14.61	0.44%	0.65	1.65	15.37
	XGB	0.48%	0.68	1.48	34.74	0.45%	0.67	1.59	19.55
	CR	0.44%	0.6	1.59	25.5	0.41%	0.68	1.74	9.11
Volatile Matter	PPR	4.45%	0.51	1.38	2.28	4.55%	0.41	1.3	7.94
	PLS	4.81%	0.42	1.27	10.65	4.45%	0.45	1.33	5.61
	RF	4.35%	0.6	1.41	0	4.21%	0.51	1.4	0
	SVM	5.02%	0.38	1.22	15.41	4.66%	0.42	1.27	10.52
	XGB	5.06%	0.36	1.21	16.23	4.45%	0.45	1.33	5.67
	CR	4.8%	0.45	1.28	10.26	4.48%	0.44	1.32	6.43
MPS	PPR	9.45 mm	0.41	1.29	16.35	5.62 mm	0.78	2.12	13.1
	PLS	8.74 mm	0.49	1.4	7.62	6.14 mm	0.75	1.94	23.48
	RF	8.12 mm	0.61	1.5	0	5.09 mm	0.83	2.34	2.44
	SVM	8.89 mm	0.48	1.37	9.44	6.29 mm	0.74	1.89	26.53
	XGB	8.17 mm	0.55	1.49	0.65	6.19 mm	0.73	1.92	24.48
	CR	8.61 mm	0.52	1.42	6.05	4.97 mm	0.82	2.39	0
Water Content	PPR	5.22%	0.61	1.61	0.8	6%	0.5	1.4	10.99
	PLS	5.6%	0.55	1.5	8.13	5.7%	0.55	1.47	5.35
	RF	5.57%	0.56	1.51	7.46	5.41%	0.6	1.55	0
	SVM	5.6%	0.58	1.5	8.18	5.9%	0.56	1.42	9.21
	XGB	7.22%	0.28	1.16	39.33	6.39%	0.47	1.31	18.13
	CR	5.18%	0.64	1.62	0	6.36%	0.5	1.32	17.67
Bulk Density	PPR	28.97 kg m^{-3}	0.53	1.44	5.57	28.47 kg m^{-3}	0.63	1.62	19.61
	PLS	31.24 kg m^{-3}	0.44	1.34	13.84	28.7 kg m^{-3}	0.62	1.6	20.57
	RF	28.3 kg m^{-3}	0.55	1.48	3.1	27.72 kg m^{-3}	0.67	1.66	16.47
	SVM	30.73 kg m^{-3}	0.52	1.36	11.97	29.94 kg m^{-3}	0.6	1.54	25.8
	XGB	31.7 kg m^{-3}	0.45	1.32	15.51	23.8 kg m^{-3}	0.73	1.93	0
	CR	27.44 kg m^{-3}	0.56	1.52	0	25.39 kg m^{-3}	0.7	1.81	6.66
P Content	PPR	0.003%	0.78	2.14	21.94	0.0032%	0.76	2.04	93.67
	PLS	0.0031%	0.82	2.07	25.8	0.0034%	0.72	1.9	107.12

Continue...

Table 4: Continuation.

		pXRF				pXRF + Auxiliary variables			
Variable	Model	RMSE	R^2	RPD	RI	RMSE	R^2	RPD	RI
	RF	0.0032%	0.75	2.03	28.42	0.0022%	0.9	2.93	34.73
	SVM	0.0025%	0.86	2.61	0	0.0038%	0.68	1.7	131.51
	XGB	0.0064%	0	1	159.67	0.0064%	0	1.01	288.88
	CR	0.0041%	0.63	1.57	65.91	0.0016%	0.94	3.94	0

MPS: mean particle size; PPR: projection pursuit regression; PLS: partial least squares; RF: random forest; SVM: support vector machine; XGB: extreme gradient boosting; and CR: cubist regression. The best results obtained for each attribute are presented in bold.

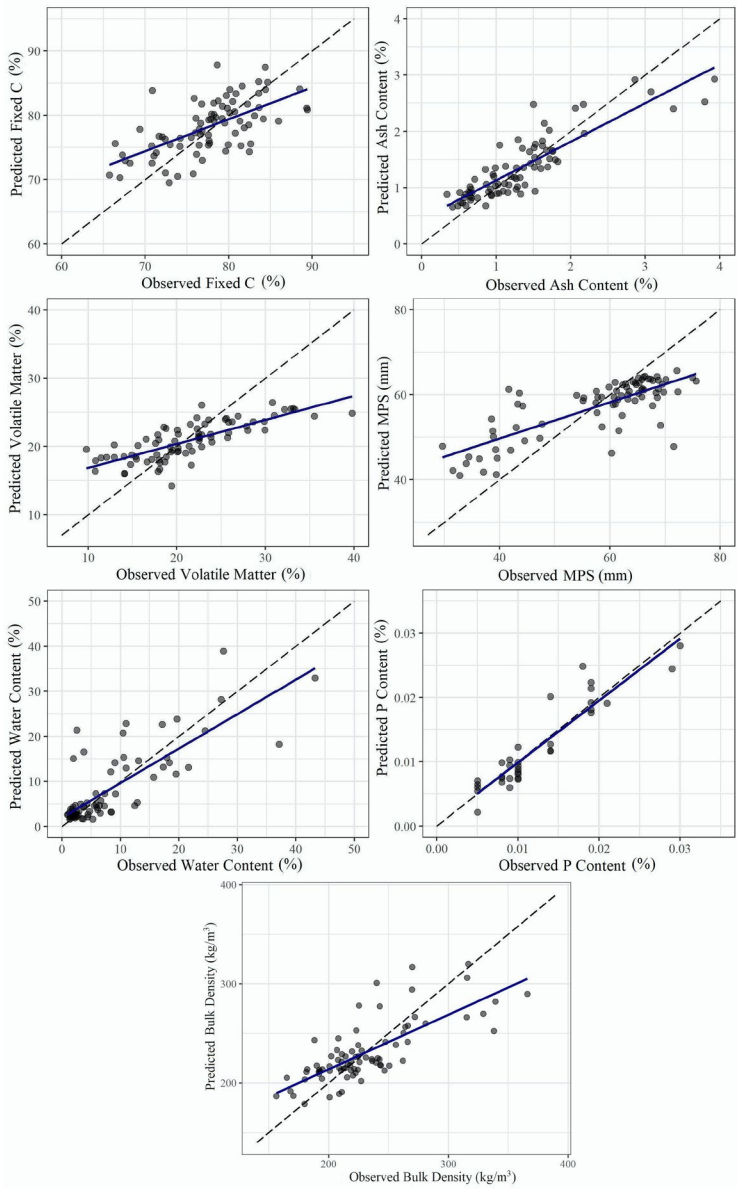

Figure 4: Independent validation of the best prediction models for fixed carbon, ashes, volatile matter, MPS, moisture, P content, and bulk density trained with portable X-ray fluorescence (pXRF) data from eucalypt charcoal samples from wood collected at the Brazilian Coastal Plains, in the state of Bahia, Brazil.

Using auxiliary variables and pXRF data

The inclusion of auxiliary variables contributed mainly to increase the accuracy of prediction models for MPS, bulk density, and P content (Table 4, Figure 6). The MPS prediction models presented R^2 values between 0.73 and 0.83, an R^2 increase of 0.18 and 0.22 compared to the respective models built only with pXRF data. The best models were built with the RF and CR algorithms (R^2 of 0.83 and 0.82, respectively). The lowest RMSE value for MPS was achieved by a CR model (4.97 mm). The increases in R^2 for bulk density predictions ranged between 0.08 and 0.29. The best performance for bulk density was achieved by the XGB algorithm, with R^2 of 0.73 and RMSE of 23.80 kg m^{-3}. Adding auxiliary variables reduced the R^2 of SVM models for P content from 0.86 to 0.68, but increased the accuracy of models built with the RF and CR algorithms. RF and CR models were capable of accurately predicting P content in eucalypt charcoal, achieving R^2 values of 0.90 and 0.94, respectively.

Accuracy increased for all tested algorithms (PPR, PLS, RF, SVM, XGB, and CR) for MPS and bulk density. However, for P content, accuracy increased only for RF and CR models, which presented high performance. Auxiliary variables contributed little to the accuracy of fixed C and volatile matter predictions, with best results achieved for XGB (R^2 = 0.46) and RF (R^2 = 0.51), respectively (Table 4, Figure 6). R^2 and RMSE values achieved by ash and water content models did not improve with the addition of auxiliary variables compared to models trained with only pXRF data. For ash and water content models trained with the inclusion of auxiliary variables, the best performing algorithm was RF.

Auxiliary variables also altered the importance of pXRF variables (Figure 5). The most important variables for fixed C predictions were: Cl > fine particle content > Sr > K > friability. For ash content: Ti > Fe > Ca > Cl > P; for volatile matter: Cl > Sr > fine particle content > P > K; for MPS: fine particle content > Fe > friability > Ti; for water content: Fe > fine particle content > Ti > Ca > Sr; for bulk density: Fe > Ti > fine particle content > wood age; and for P content: wood age > K > drying time > Cl > Si. The auxiliary variables fine particle content and wood age substantially contributed to the improvement of models. Fine particle content appeared five times in the selected group of important variables and was also the most important variable for MPS predictions, the second most important for fixed C and water content predictions, and the third most important for volatile matter and bulk density predictions. Wood age was the most important variable for P content predictions, which presented the highest R^2 value (Table 4). The most noteworthy changes in variable importances after adding auxiliary variables were: the order between Fe and Ti for ash content models, the decrease in importance of Si in MPS models, the decrease in importance of Fe for water content models, and decrease in importance of K, Cl, and P for P content models.

Ash is the residual mineral material in a sample after burning. Therefore, there is a relationship between ash contents and the contents of mineral elements (considering the loss of C, O, N, H, and S) (Somprasong et al., 2018), which were shown by PCA analysis. For instance, PCA analysis showed correlation between the ash content and Ca data, and between Fe and Sr, ranked as important variables by models (Figures 2 and 4). P content was correlated to K, Cl, and P, the most important variables for P content prediction models. The addition of auxiliary variables that are correlated with predicted attributes is known to increase the accuracy of models (Swanhart et al., 2014; Sharma et al., 2015; Stiglitz et al., 2018; Pelegrino et al., 2019; Lima et al., 2023; Dasgupta et al., 2022;2024; Andrade et al., 2022; Dijair et al., 2020). The relationships shown by the PCA therefore help explain the observed accuracy improvements.

The relationship between friability, fine particle content, and bulk density shown by PCA (Figure 2) can be explained by the influence of particle size on density. Friability increases with fine particle content (Dufourny et al., 2019), and granulometry exerts a strong influence on bulk density, as smaller pieces increase the mass of charcoal that can fit in a container per volume (Dias Júnior et al., 2021). Water present in the sample (drying time) and the age of the plant has a large influence in P content found in the wood, and consequently in the resulting charcoal (Figure 2) (Turner & Lambert, 2008). Since phosphate fertilization of forest species is mainly supplied when planting the seedlings, it is likely that the levels of P in eucalypt plants are higher at early development stages and decrease with time (Godoi et al., 2021). Therefore, caution is warranted when using young eucalypt trees to produce charcoal, as high P levels in eucalypt charcoal can negatively affect the quality of the produced pig iron (Rodrigues et al., 2016; Dong et al., 2022).

The relative importance showed comparatively the effect of auxiliary variables in reducing prediction error (Figure 7). Models using pXRF data alone obtained higher accuracy for fixed C (PPR), ash content, and water content (CR). The addition of auxiliary variables resulted in an increase in prediction accuracy for volatile matter (RF), MPS (CR), bulk density (XGB), and P content (CR). Another important point to consider when including auxiliary variables is their availability or ease of acquisition (Tavares et al., 2023).

Auxiliary variables must be easy to obtain, whether through laboratory analyses, observations, or tabulated data, in addition to being consistent. The inclusion of auxiliary variables should contribute to the performance of models without bringing new challenges or causing model overfiting. As such, fine particle content and wood age, which were considered very important by models (Figure 5), were the most promising auxiliary variables due to their ease of acquisition and their contributions to model performance.

Applicability of prediction models for the quality control of charcoal

Positive results obtained in this study indicate that pXRF data has great potential to accurately predict P and ash contents in eucalypt charcoal (R^2 of 0.94 and 0.75, respectively) (Table 4, Figure 4), contributing to facilitate the quality control of charcoal used in the steel industry. To produce high-quality pig iron, it is important to guarantee that the charcoal has low ash and P contents, as ashes and P increase the brittleness of pig iron, with

zones prone to developing cracks and fissures (Santos et al., 2016). High ash content causes wear in the blast furnace and can affect the quality of pig iron due to the segregation phenomenon (Pereira et al., 2012; Carnaje et al., 2018). In adequate concentrations, the presence of P in the interstitial-free steel can improve drawability by promoting a favorable texture, hot ductility of low-alloy steel, and atmospheric corrosion resistance of weathering steels (Ray, Ghosh, & Bhattacharjee, 2009; Jiang et al., 2013; Song et al., 2014; Dong et al., 2022). However, excess P can lead to phosphorus segregation on austenite grain boundaries, increasing brittleness and reducing the toughness and corrosion resistance of the metal (Rodrigues et al., 2016; Dong et al., 2022).

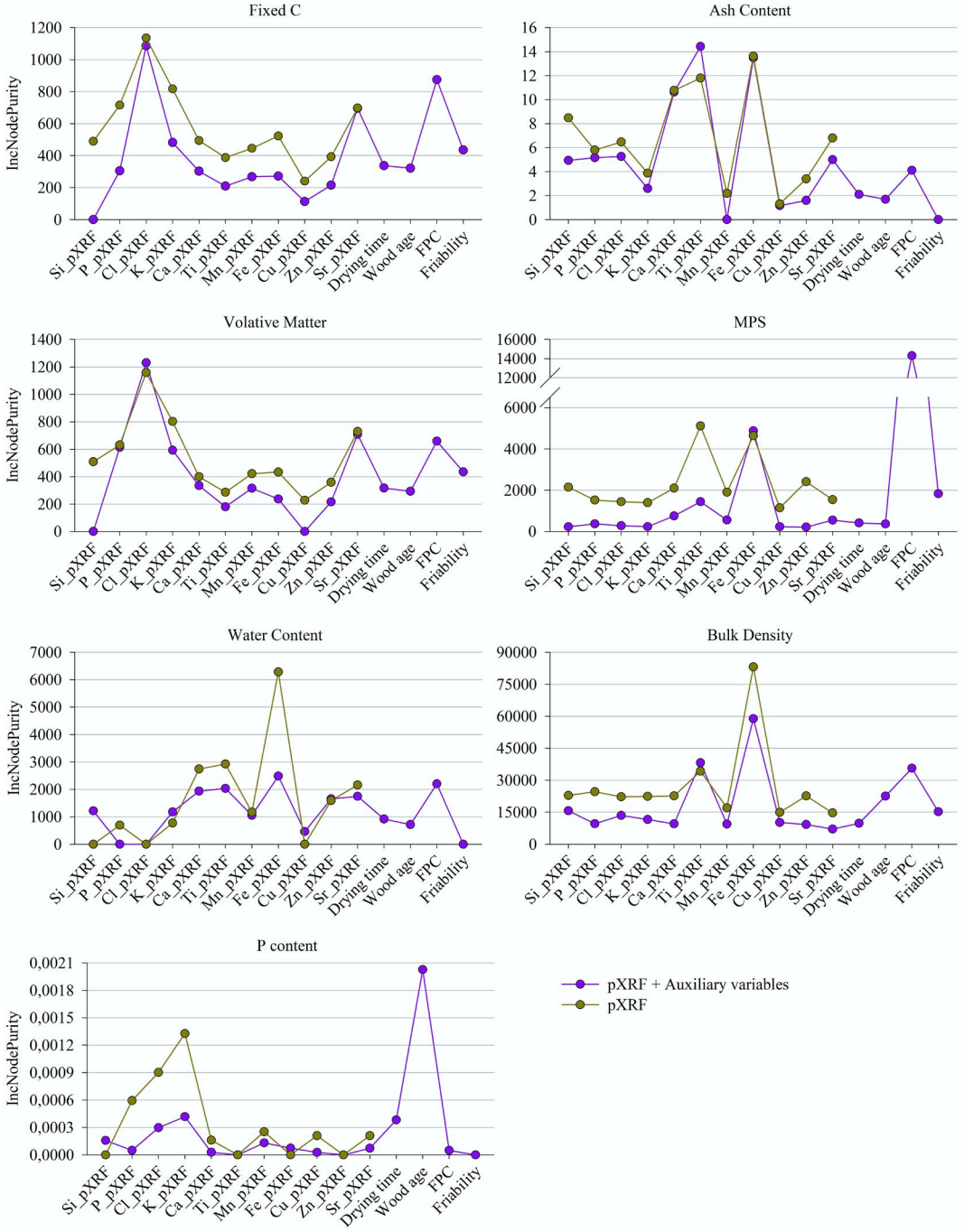

Figure 5: Variable importance for prediction models of eucalypt charcoal attributes built with pXRF data with and without auxiliary variables: drying time, wood age, fine particle content (FPC), and friability. Charcoal samples were made from eucalypt wood collected at the Brazilian Coastal Plains, in the state of Bahia, Brazil.

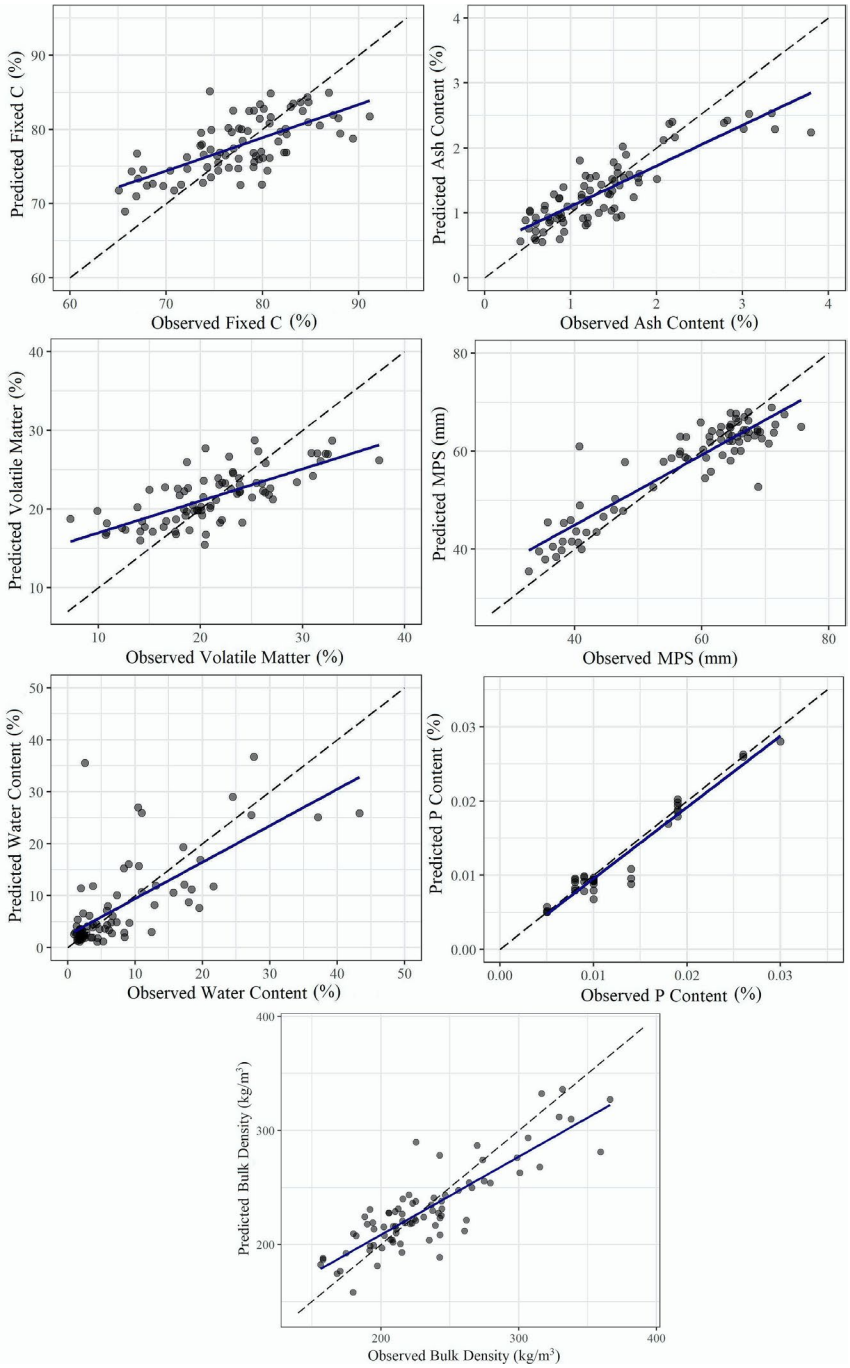

Figure 6: Independent validation of the best prediction models for fixed C, ash content, volatile matter, MPS, water content, P content, and bulk density in eucalypt charcoal samples. Models were trained with portable X-ray fluorescence (pXRF) data and auxiliary variables (drying Time, wood age, fine particle content, and friability). Charcoal samples were made from eucalypt wood collected at the Brazilian Coastal Plains, in the State of Bahia, Brazil. The 1:1 line is represented by the dashed line.

With the inclusion of auxiliary variables, MPS and bulk density were accurately predicted (R^2 of 0.83 and 0.73, respectively) (Table 4, Figure 5). For high-quality eucalypt charcoal, it is desirable that its density value would not be < 0.40 g cm^{-3}. Low density values limit the amount of fixed C available in the furnace for carbothermic reactions, reducing productivity and increasing energy consumption (Dufourny et al., 2019). Conversely, high MPS are desirable, as small particles would result in low gas permeability in the furnace, impairing the efficiency of metallurgical reactions (Assis et al., 2020).

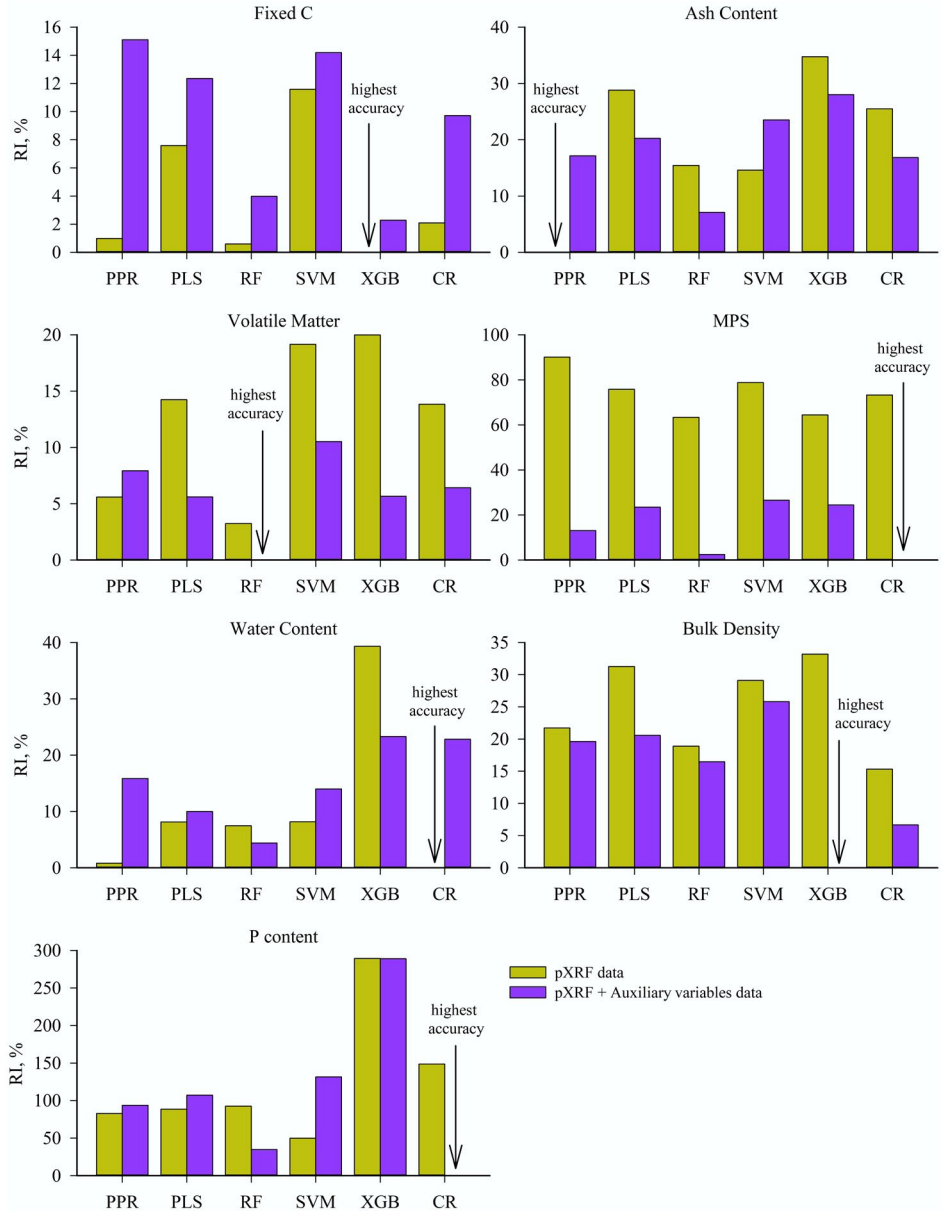

Figure 7: Relative increase (RI) of root mean squared error *(*RMSE*)* values of models built with portable X-ray fluorescence *(*pXRF*)* data alone and with the inclusion of auxiliary variables for each predicted attribute of eucalypt charcoal, using the model with the lowest RMSE (highest accuracy) as a reference. Charcoal samples were made from eucalypt wood collected at the Brazilian Coastal Plains, in the state of Bahia, Brazil.

Therefore, rapid, low-cost, ecofriendly and non-destructive pXRF analysis can facilitate the accurate quality assessment of eucalypt charcoal used in the steel industry, aiding in decision-making. In traditional laboratory analyses of eucalypt charcoal (ASTM, 2021), P content is obtained through digestion in nitric acid (HNO_3) prior to quantification by ICP-OES. Some methods of bulk density analysis involve immersing samples in mercury, such as the hydrostatic method. These analyses are accurate and well-established, but they must be performed in appropriate locations, requiring calibrated equipment and hazardous chemical reagents. These hazardous wastes require a suitable location for their disposal (Benedet et al., 2021). In addition, these analyses demand considerable time and are very expensive. Cost and time can be reduced by pXRF analysis. Efficient quality assessment can contribute to greater safety in industrial processes by enabling the analysis of more samples without increasing cost. However, it is important to emphasize that the pXRF assessment is not meant to replace the well-

established methods of analysis. Proximal sensor analysis has the primary objective of substantially decreasing the number of samples that undergo traditional analyses (which will continue to be the reference for prediction models). Proximal sensing methods aim to support fast and accurate decision-making in steel industries based on careful statistical validation performed using data from conventional and precise laboratory methods. These methods can be expanded and tested on other important parameters used to assess the quality of charcoal.

The use of sensor technology paired with sound modeling methods can be a game changer in the monitoring of charcoal quality. We advise further testing with charcoal samples with different levels of quality and possibly other attributes of interests. Complimentary studies using charcoal made with wood from clones and species are also recommended as a future effort, as they will help better understanding the extent to which pXRF can be useful for the steel industry, or even for other important production chains. The fast and accurate prediction of ash and P Content via proximal sensing is a promising alternative to facilitate the quality control of eucalypt charcoal and could be extended in the future to other key charcoal attributes.

Conclusions

Models trained with only pXRF data achieved accurate predictions for most variables, especially for ash and P contents. The exceptions were fixed C models, which did not achieve satisfactory accuracy. The inclusion of auxiliary explanatory variables, especially fine particle content and wood age, increased the prediction accuracy of MPS, bulk density, and P content. PXRF analyses represent an ecofriendly methodology capable of speeding up the quality assessment of eucalypt charcoal used by the steel industry.

Authors contributions

Conceptual idea: Silva, S.H.G.; Freitas, C.S.; Carneiro, M.A.C; Curi, N.; Methodology design: Silva, S.H.G.; Curi, N.; Data collection: Freitas, C.S.; Data analysis and interpretation: Andrade, R.; Benedet., L.; Silva, S.H.G.; and Writing and editing: Andrade, R.; Benedet, L; Mancini, M.; Silva, S.H.G.; Freitas, C.S.; Curi, N.

Acknowledgments

The authors would like to thank the National Council for Scientific and Technological Development (CNPq), the Coordination for the Improvement of Higher Education Personnel (CAPES), and the Research Foundation of the State of Minas Gerais (FAPEMIG) for the financial support to develop this research.

References

Al Hosni, S. et al. (2024). Potential and environmental benefits of biochar utilization for coal/coke substitution in the steel industry. *Energies*, *17*(11):2759

Assis, M. R. et al. (2020). Towards a better understanding of the mechanical behavior of a fixed bed of eucalyptus charcoal in a blast furnace using a specific compression test. *BioResources*, *15*(4):7660.

American Society for Testing and Materials - ASTM. (2021). *Standard test method for chemical analysis of wood charcoal*. Available in: <https://www.astm.org/d1762-84r21.html>

Acquah, G. E. et al. (2022). Portable X-ray fluorescence (pXRF) calibration for analysis of nutrient concentrations and trace element contaminants in fertilisers. *PLOS ONE*, *17*:e0262460.

Andrade, R. et al. (2020). Prediction of soil fertility via portable X-ray fluorescence (pXRF) spectrometry and soil texture in the Brazilian Coastal Plains. *Geoderma*, *357*:113960.

Andrade, R. et al. (2022). Proximal sensor data fusion and auxiliary information for tropical soil property prediction: Soil texture. *Geoderma*, *422*:115936.

Andrade, R. et al. (2023a). A proximal sensor-based approach for clean, fast, and accurate assessment of the Eucalyptus spp. nutritional status and differentiation of clones. *Plants*, *12*(3):561.

Andrade, R. et al. (2023b). Proximal sensing provides clean, fast, and accurate quality control of organic and mineral fertilizers. *Environmental Research*, *236*:116753.

Benedet, L. et al. (2020a). Soil subgroup prediction via portable X-ray fluorescence and visible near-infrared spectroscopy. *Geoderma*, 365:114212.

Benedet, L. et al. (2021). Rapid soil fertility prediction using X-ray fluorescence data and machine learning algorithms. *Catena*, *197*:105003.

Benedet, L. et al. (2023). Clean quality control of agricultural and non-agricultural lime by rapid and accurate assessment of calcium and magnesium contents via proximal sensors. *Environmental Research*, *221:*115300.

Breiman, L. (2001). Random forests. *Machine Learning*, *45*:5-32.

Carnaje, N. P. et al. (2018). Development and characterisation of charcoal briquettes from water hyacinth (*Eichhornia crassipes*)-molasses blend. *PloS One*, *13*(11):e0207135.

Chang, C. W. et al. (2001). Near-infrared reflectance spectroscopy–principal components regression analyses of soil properties. *Soil Science Society of America Journal*, *65*(2):480-490.

Chen, T., & Guestrin, C. (2016). XGBoost: A scalable tree boosting system. *Proceedings of the 22nd ACM SIGKDD International Conference on Knowledge Discovery and Data Mining*, 785-794.

Cortes, C., & Vapnik, V. (1995). Support-vector networks. *Machine Learning*, *20*(3):273-297.

Dasgupta, S. et al. (2022). Influence of auxiliary soil variables to improve PXRF-based soil fertility evaluation in India. *Geoderma Regional*, *30*:e00557.

Dasgupta, S. et al. (2024). Soil fertility prediction using combined USB-microscope based soil image, auxiliary variables, and portable X-ray fluorescence spectrometry. *Soil Advances*, *2*:100016.

Dias Júnior, A. F. et al. (2021). Blends of charcoal fines and wood improve the combustibility and quality of the solid biofuels. *BioEnergy Research*, *14*:344-354.

Dijair, T. S. B. et al. (2020). Correcting field determination of elemental contents in soils via portable X-ray fluorescence spectrometry. *Ciência e Agrotecnologia*, *44:*e002420.

Dong, F. et al. (2022). The influence of phosphorus on the temper embrittlement and hydrogen embrittlement of some dual-phase steels. *Materials Science and Engineering: A*, *854:*143379.

Dufourny, A. et al. (2019). Influence of pyrolysis conditions and the nature of the wood on the quality of charcoal as a reducing agent. *Journal of Analytical and Applied Pyrolysis*, *137:*1-13.

Empresa de Pesquisa Energética - EPE (2023). *Balanço energético anual*. Available in: https://www.epe.gov.br/sites-pt/publicacoes-dados-abertos/publicacoes/PublicacoesArquivos/publicacao-748/topico-687/BEN2023.pdf

Faria, Á. J. G. et al. (2020). Soils of the Brazilian Coastal Plains biome: Prediction of chemical attributes via portable X-ray fluorescence (pXRF) spectrometry and robust prediction models. *Soil Research*, *58*(7):683.

Frank, l. E., & Friedman, J. H. (1993). A statistical view of some chemometrics regression tools. *Technometrics*, *35*(2):109-135.

Friedman, J. H., & Stuetzle, W. (1981). Projection pursuit regression. *Journal of the American Statistical Association*, *76*(376):817-823.

Godoi, N. M. I. et al. (2021). Residual influence of nitrogen, phosphorus and potassium doses on soil and eucalyptus nutrition in coppice. *Forests*, *12*(10):1462.

Holappa, L. (2020). A general vision for reduction of energy consumption and CO2 emissions from the steel industry. *Metals*, *10*(9):1117.

Indústria Brasileira de Árvores - IBA (2023). *Relatório Annual 2023*. Available in: <https://iba.org/datafiles/publicacoes/relatorios/relatorio-anual-iba2023-r.pdf>

Instituto Brasileiro de Mineração - IBRAM. (2021). *Programa siderurgia sustentável permite que o carvão vegetal seja o principal combustível de grandes siderúrgicas*. Available in: https://ibram.org.br/noticia/siderurgias-utilizam-carvao-vegetal-como-principal-combustivel/#:~:text=O%20carv%C3%A3o%20vegetal%2C%20al%C3%A9m%20de,projeto%20ser%C3%A1%20conclu%C3%ADdo%20em%202021

Jiang, X. et al. (2013). Phosphorus-induced hot ductility enhancement of 1Cr–0.5 Mo low alloy steel. *Materials Science and Engineering: A*, *574:*46-53.

Jolliffe, I. T., & Cadima, J. (2016). Principal component analysis: A review and recent developments. *Philosophical Transactions of the Royal Society A: Mathematical, Physical and Engineering Sciences*, *374*:2065.

Kagiliery, J. et al. (2019). Rapid quantification of lignite sulfur content: Combining optical and X-ray approaches. *International Journal of Coal Geology*, *216*:103336.

Koch, J. et al. (2017). Proximal sensor analysis of mine tailings in South Africa: An exploratory study. *Journal of Geochemical Exploration*, *181*:45-57.

Kursa, M. B., & Rudnicki, W. R. (2010). Feature selection with the boruta package. *Journal of Statistical Software*, *36*(11):1-13.

Kuhn, M. et al. 2012. Cubist models for regression. Available in: https://rdrr.io/rforge/Cubist/f/inst/doc/cubist.pdf

Kuhn, M. (2008). Building predictive models in R using the caret package. *Journal of Statistical Software*, *28*(5), Article 5.

Liaw, A., & Wiener, M. (2002). Classification and regression by random forest. *R News*, *2*(3):18-22.

Lima, F. R. D. et al. (2023). Predictive modeling of total Hg background concentration in soils of the Amazon Rainforest biome with support of proximal sensors and auxiliary variables. *Journal of South American Earth Sciences*, *129*:104510.

Ministério da Indústria, Comércio Exterior e Serviços -MDIC. (2024). *Carvão, mesmo em pó, mas não aglomerado. Comexstat*. Available in: https://comexstat.mdic.gov.br/pt/comex-vis/4/321.

Mousa, E. et al. (2016). Biomass applications in iron and steel industry: An overview of challenges and opportunities. *Renewable and Sustainable Energy Reviews*, *65*:1247-1266.

Pelegrino, M. H. P. et al. (2019). Synthesis of proximal sensing, terrain analysis, and parent material information for available micronutrient prediction in tropical soils. *Precision Agriculture*, *20*:746-766.

Oliveira, L. P. D. et al. (2023). Wood and charcoal quality in the selection of eucalyptus spp. clones and *Corymbia torelliana* X *corymbia* citriodora for steel industry. *Revista Árvore*, *47:*e4722.

Pereira, B. L. C. et al. (2012). Quality of wood and charcoal from eucalyptus clones for ironmaster use. *International Journal of Forestry Research*, *523025*, 8 pages.

Protásio, T. P. et al. (2021). Charcoal productivity and quality parameters for reliable classification of *Eucalyptus* clones from Brazilian energy forests. *Renewable Energy*, *164:*34-45.

Protásio, T. P. et al. (2019). Assessing proximate composition, extractive concentration, and lignin quality to determine appropriate parameters for selection of superior *Eucalyptus* firewood. *BioEnergy Research*, *12*:626-641.

R Development Core Team. (2021). R*: A language and environmental for statistical computing*. R Foundation for Statistical Computing, Vienna, Austria. Available in: <https://www.R-project.org/>.

Ramalho, F., Gherardi Hein, P. R., Napoli, A., Wojcieszak, R., & Guilherme, L. (2020). Artificial neural networks to distinguish charcoal from *Eucalyptus* and native forests based on their mineral components. *Energy & Fuels*, *34*.

Ray, R. K., Ghosh, P., & Bhattacharjee, D. (2009). Effects of composition and processing parameters on precipitation and texture formation in microalloyed interstitial free high strength (IFHS) steels. *Materials Science and Technology*, *25*(9):1154-1167.

Rodrigues, C. A. D. et al. (2016). Effect of phosphorus content on the mechanical, microstructure and corrosion properties of supermartensitic stainless steel. *Materials Science and Engineering: A*, *650*:75-83.

Rosin, N. A. et al. (2022). The fundamental of the effects of water, organic matter, and iron forms on the pXRF information in soil analyses. *Catena*, *210*:105868.

Santos, R. C. et al. (2016). Effect of properties chemical and siringil/guaiacil relation wood clones of *Eucalyptus* in the production of charcoal. *Ciência Florestal*, *26*(2):657-669.

Sharma, A. et al. (2015). Characterizing soils via portable X-ray fluorescence spectrometer: 4. Cation exchange capacity (CEC). *Geoderma*, *239*:130-134.

Silva, S. H. G. et al. (2021). Chapter one - pXRF in tropical soils: Methodology, applications, achievements and challenges. In D. L. Sparks (Ed.). *Advances in Agronomy*. London, England: Academic Press, v.167, (pp.1-62).

Silva, F. T. M., & Ataíde, C. H. (2019). Valorization of eucalyptus urograndis wood via carbonization: Product yields and characterization. *Energy*, *172*:509-516.

Sindicato da Indústria do Ferro no Estado de Minas Gerais – SINDIFER. (2024). *Anuário estatístico, ano base 2023*. Available in: <https://sindifer.com.br/sndfr/anuario-estatistico/>

Sociedade de Investigações Florestais -SIF. (2020). *Importância do uso do carvão vegetal pelo setor de metalurgia e siderurgia e a balança comercial brasileira.* Available in: <https://sif.org.br/2020/04/importancia-do-uso-do-carvao-vegetal-pelo-setor-de-metalurgia-e-siderurgia-e-a-balanca-comercial-brasileira/>.

Somprasong, K., Thiteja, S., & Jaroonpattanapong, P. (2018). Introductory to the application of portable X-Ray fluorescent spectroscopy (PXRF) on the Investigation of on-site ash content analysis. *International Journal of Electronics and Electrical Engineering*, *6*(2):10-15.

Song, X. L. et al. (2014). Texture, grain boundary characterization and segregation of phosphorus in an annealed interstitial free steel. *Journal of Iron and Steel Research International*, *21*(9):844-848.

Stiglitz, R. Y. et al. (2018). Predicting soil organic carbon and total nitrogen at the farm scale using quantitative color sensor measurements. *Agronomy*, *8*(10):212.

Swanhart, S. et al. (2014). Soil salinity measurement via portable X-ray fluorescence spectrometry. *Soil Science*, *179*(9):417.

Tavares, T. R. et al. (2023). Analysis of total soil nutrient content with X-ray fluorescence spectroscopy (XRF): Assessing different predictive modeling strategies and auxiliary variables. *AgriEngineering*, *5*(2):680-697.

Tomczyk, C., & Larousse, M. N. (2024). Efficiency of portable X-ray fluorescence for distinguishing lead slag. *Applied Spectroscopy*, *78*(2):175-185.

Turner, J., & Lambert, M. J. (2008). Nutrient cycling in age sequences of two eucalyptus plantation species. *Forest Ecology and Management*, *255*(5-6):1701-1712.

Ward, C. R. et al. (2018). In-situ inorganic analysis of coal seams using a hand-held field-portable XRF Analyser. *International Journal of Coal Geology*, *191*:172-188.

Weindorf, D. C., Bakr, N., & Zhu, Y. (2014). Advances in portable X-ray fluorescence (PXRF) for environmental, pedological, and agronomic applications. *Advances in Agronomy*, *128*:1-45.

Weindorf, D. C., & Chakraborty, S. (2018). Portable apparatus for soil chemical characterization. U.S. Patent No. 10107770, 23 October 2018. Available in: <https://pubchem.ncbi.nlm.nih.gov/patent/US-10107770-B2>.

Zhou, S. et al. (2020). Quantitative analysis of iron and silicon concentrations in iron ore concentrate using portable X-ray fluorescence (XRF). *Applied Spectroscopy*, *74*(1):55-62.